Available online at www.sciencedirect.com
ScienceDirect
International Journal of Heat and Mass Transfer 49 (2006) 4910–4920
International Journal of HEAT and MASS TRANSFER
www.elsevier.com/locate/ijhmt

Spray cooling of enhanced surfaces: Impact of structured surface geometry and spray axis inclination

Eric A. Silk [a,*], Jungho Kim [b], Ken Kiger [b]

[a] Thermal Engineering Technology Development Group, NASA Goddard Space Flight Center, Greenbelt, MD 20771, United States
[b] Phase Change Heat Transfer and Multiphase Transport Laboratories, Mechanical Engineering Department, University of Maryland, College Park, MD 20742, United States

Received 23 January 2006; received in revised form 24 May 2006
Available online 9 August 2006

Abstract

Experiments were conducted to study the effects of enhanced surfaces and spray inclination angle (the angle between the surface normal and the axis of symmetry of the spray) on heat transfer during spray cooling. The surface enhancements consisted of cubic pin fins, pyramids, and straight fins. These structures were machined on the top surface of heated copper blocks with 2.0 cm^2 cross-sectional areas. Measurements were also obtained on a heated flat surface to provide baseline data. PF-5060 was used as the working fluid. The spray was produced using a 2×2 nozzle array under nominally degassed conditions (chamber pressure of 41.4 kPa) with a volume flux of 0.016 m^3/m^2 s and a nozzle height of 17 mm. The spray temperature was 20.5 °C. For the geometries tested, the straight fins had the largest heat flux enhancement relative to the flat surface, followed by the cubic pin fins and the pyramid surface. Each of these surfaces also indicated an increase in evaporation efficiency at CHF compared to the flat surface. Inclination of the spray axis between 0° and 45° relative to the heater surface normal created a noticeable increase in heat flux compared to the normal position (0° case). A maximum heat flux enhancement of 23% was attained for the flat surface. The straight finned surface had a maximum heat flux enhancement of 75% at an inclination angle of 30° relative to the flat surface in the normal position. However, only a marginal increase (~11%) was observed in comparison to the straight finned surface in the normal position (0° case).

Keywords: Enhancement; Spray cooling; Finned surfaces; Heat transfer

1. Introduction

1.1. Background

NASA's new vision for space exploration encompasses the development of alternative power systems and advanced on-board flight system components such as laser–diode arrays (LDA's) and multi-chip modules (MCM's). Thermal management of these systems is critical to mission success. Projected thermal control requirements include high heat flux cooling capability ($\geqslant 100$ W/cm^2), tight temperature control (approx +/−2 °C), reliable (on demand) start-up, shut down, and long term stability. Traditional multiphase thermal control flight technologies (loop heat pipes, capillary pumped loops, etc.) satisfy the temperature control and stability requirements, but their heat flux removal capabilities are limited. Spray cooling can provide high heat fluxes in excess of 100 W/cm^2 using fluorinerts and over 1000 W/cm^2 with water while allowing tight temperature control at low coolant fluid flow rates. It is a proven flight technology that has been demonstrated through the Space Shuttle's open loop flash evaporator system (FES). Provided closed system issues such as scavenging excess liquid and vapor can be adequately resolved, spray cooling presents one of the most appealing heat transfer techniques for the thermal management needs of tomorrow's high heat flux space platforms. As with any

* Corresponding author.
E-mail address: Eric.A.Silk@nasa.gov (E.A. Silk).

0017-9310/$ - see front matter © 2006 Elsevier Ltd. All rights reserved.
doi:10.1016/j.ijheatmasstransfer.2006.05.031

Nomenclature

A	area
H	structure height
L	distance between successive structures
P	pressure
R_a	surface roughness
R_{fl}	$\frac{(T_{surf}-T_l)}{\dot{q}''}$, convective thermal resistance
T	temperature
TC	thermocouple
X	structure feature dimension
c_p	specific heat
h	convection coefficient
h_{fg}	enthalpy of vaporization
k	conductivity
$\dot{m}$	mass flow rate
p	structure pitch
$\dot{q}''$	heat flux per unit area
u	uncertainty
x	distance from heater surface within heater
ΔP	pressure across nozzle
Γ	weighted volume flux for concentric ring
$\delta\dot{q}''$	error in heat flux
δ_k	error in conductivity
$\delta_{\Delta T}$	error in thermocouple temperature difference
δ_x	error in thermocouple location
η	evaporation efficiency
ξ	area utilization factor, $(q''_{surf}/q''_{flat})/(A_{surf}/A_{flat})$

Subscripts

flat	flat surface
i	concentric ring
k	conductivity
l	liquid
CHF	critical heat flux
max	maximum
sat	saturation conditions
surf	surface
T	temperature
x	thermocouple distance
$1-\Phi$	single phase
$2-\Phi$	multiphase

emerging thermal management technology, finding ways to increase the thermal performance through passive enhancement mechanisms can offer substantial benefits, and is the focus of the current work.

1.2. Literature review

1.2.1. General studies

Many research efforts have been performed to gain a better understanding of the phenomena and critical parameters associated with spray cooling heat transfer. A review of the literature shows that previous studies have parametrically examined the effect of secondary gas atomizers vs. pressure atomizers [1,2], mass flux of ejected fluid [3,4], spray velocity [5,6], surface impact velocity [5–8], microscale surface roughness [1,6,9,10], ejected fluid temperature [11], chamber environmental conditions [11], and spray footprint optimization on the effective heat flux across the heater surface [11]. Other topics researched to date include the effect of surfactant addition [12,13], secondary nucleation [1,14,15] and dissolved gas effects [16].

1.2.2. Surface roughness

Spray cooling is considered a multiphase convective process, and is subject to traditional heat transfer enhancement techniques that are typically applied to convective heat exchange surfaces. While the Space Shuttle's FES used cyclic water spray cooling of enhanced surfaces (triangular grooves) to cool freon based heat exchangers [17], overall work in the area of spray cooling with enhanced surfaces has been very limited. Most previous studies that have examined enhanced surfaces have done so primarily from the perspective of surface roughness. Sehmbey et al. [1] gives an overview of spray cooling and provides a comparison of its effectiveness when using liquid and secondary gas atomizers (air used as the secondary gas). Heat flux was measured and presented for both techniques. It was found that the heat transfer coefficient increased with the use of smooth surfaces ($R_a < 0.1$ μm) for gas atomized sprays, while the opposite trend was observed for liquid atomized sprays. Both the heat flux and the convection coefficient were found to have comparable values for both atomizer types. The authors concluded that the most important parameters affecting heat transfer were the fluid properties, spray velocity, and surface roughness.

Pais et al. [10] studied the effects of surface roughness (values ranged 0.3–22.0 μm) on heat transfer when using spray cooling. The sprayed surface was copper with a projected area of 1 cm^2. An air-assist atomizing nozzle was used with deionized water as the working fluid. Tests were conducted at a nozzle height of 23 mm. It was found that the 0.3 μm surface achieved the highest heat flux, with a peak heat flux of 1250 W/cm^2. The onset of nucleate boiling also occurred at lower superheat values. The authors attributed the heat transfer enhancement to early bubble departure from the surface during nucleate boiling, and concluded that secondary nucleation has a primary role as a heat transfer mechanism only if the surface finish is smooth.

1.2.3. Enhanced surface pool boiling

Much work has been performed on pool boiling using enhanced surfaces. Surface modifications previously investigated include the use of paints, porous structures, and structured surface geometries (submicron, micro, and

macro). Each of these techniques has been shown to enhance heat transfer under certain conditions. Honda et al. [18] investigated FC-72 boiling on silicon chips with micro-pin-fins, submicron-scale roughness, and a surface utilizing a combination of both enhancements. The square pins had dimensions of $50 \times 50 \times 60\ \mu m^3$, while the submicron-scale roughened surface had a root mean square (RMS) roughness between 25 and 32 nm. The effects of subcooling and dissolved gas on heat flux were reported for each of these surfaces. The submicron-scale roughened surface displayed a higher heat transfer than the micro-pin-finned surface at low heat flux. The opposite trend was observed at high heat flux. The combination surface displayed the highest heat transfer of the surfaces tested with a CHF value 1.8–2.3 times larger than the corresponding smooth surface case. CHF was found to vary linearly with subcooling for all chips.

Chien and Webb [19] investigated the effects of structured tunnel dimensions on nucleate boiling convection coefficients for heat fluxes ranging from 2–70 kW/m^2. Tests were performed on a 19.1 mm diameter horizontal tube using R-11 and R-123 as working fluids. Tunnel pitch, height, width, and base radius were the primary dimensions studied. The authors found that fins shorter than 0.9 mm experienced significant increases in the convection coefficient as the fin count increased from 1378 to 1575 fins/m. They also found that straight fins promoted increased evaporation by retaining more liquid between neighboring fins. Increased fin height had little effect upon the convection coefficient. Fin pitch was also observed to have little effect.

1.2.4. Spray inclination angle

Previous investigations with the spray axis inclined relative to the heater surface normal have typically emphasized their impact upon heat flux via removal of residual liquid on the heat exchange surface. Shedd and Pautsch [20] used inclined sprays to assist with fluid drainage and provide orientation-independent heat flux performance. Mudawar and Estes [11] examined heat flux as a function of cone angle and nozzle height for a given flow rate. The heater test surface was square ($12.7 \times 12.7\ mm^2$) while the nozzle had a circular spray footprint. The working fluids were FC-72 and FC-87. The authors determined that CHF was a function of volumetric flow distribution on the heater surface. The optimum CHF was attained when the spray cone footprint was inscribed within the perimeter of the heater surface.

Kearns et al. [21] studied spray cooling of a row of heaters inside a narrow channel. A total of nine heaters were used, each with an area of 38.1 mm^2. The channel length, width, and height were 400, 265, and 255 mm, respectively. Fluid was sprayed into the channel at one end by a single full cone nozzle with a cone angle of 55°. The configuration was designed to simulate the confined conditions inside a row of circuit boards. The working fluid was PF-5060 at 101 kPa. Maximum heat dissipation (60 W) occurred with the heater closest to the nozzle, while the minimum dissipation (20 W) occurred on the heater farthest away. The authors concluded that this was due to the proximity of the leading heater relative to the nozzle as well as the impingement angle on its leading edge.

Schwarzkopf et al. [22] studied the effect of spray inclination angle on spray cooling using a single atomizer. The heated surface consisted of a thermal test chip with multiple heater modules, each of which contained an embedded temperature sensor. The heated surface was mounted in an upside down (heater normal facing downwards) configuration. The fluid was sprayed upward onto the heated surface. Spray angles varied between 0° and 60° (spray axis measured relative to the heater normal) with the orifice kept at a constant radius of 1.4 cm from the heated surface. The working fluid used was PF-5060 at 101 kPa. The authors showed that CHF was $\approx 63\ W/cm^2$ for inclination angles between 0° and 40°. CHF decreased rapidly for spray inclination angles greater than 40°.

1.2.5. Objectives of present work

The objective of the current work is to examine the effects of structured surface geometries that are much larger than the liquid film thickness on spray cooling performance. This is the first study of its kind and illustrates that enhanced surfaces can provide significantly larger heat transfer relative to smooth surfaces. Three enhanced surface geometries (cubic pin fins, pyramids, and straight fins) were tested to determine heat flux as a function of surface geometry. The flat surface and the enhanced surface geometry with the highest CHF were tested further to determine the impact of spray axis inclination angles between 0° and 45°.

2. Experimental apparatus and data reduction

2.1. Test set-up

The experiments were conducted within a closed fluid loop. The test rig (schematic shown in Fig. 1) consisted of a test chamber, pump, flow meter, micro-filter, and a condenser. Chamber temperature and pressure were measured using a T-type thermocouple and a pressure sensor. Temperature and pressure sensors were also placed in the liquid line directly upstream of the nozzle to measure liquid supply line temperature and the pressure across the nozzle.

Instrumented test blocks were constructed with the different enhanced geometries machined directly on their top surface. The blocks were made of oxygen-free high conductivity copper. A uniform undercoat of nickel (2.54 μm thickness) was deposited to minimize diffusion of the topcoat into the copper. A gold topcoat was applied (1.27 μm thickness) to provide a stable (non-oxidizing) surface with sufficient durability to last throughout the experiments. Heat was supplied to the test surfaces using a 500 W cartridge heater. The heater assembly was placed within the interior of the chamber, but was separated from the excess liquid by an enclosure consisting of a polycarbonate housing and an alumina bisque ceramic top flange

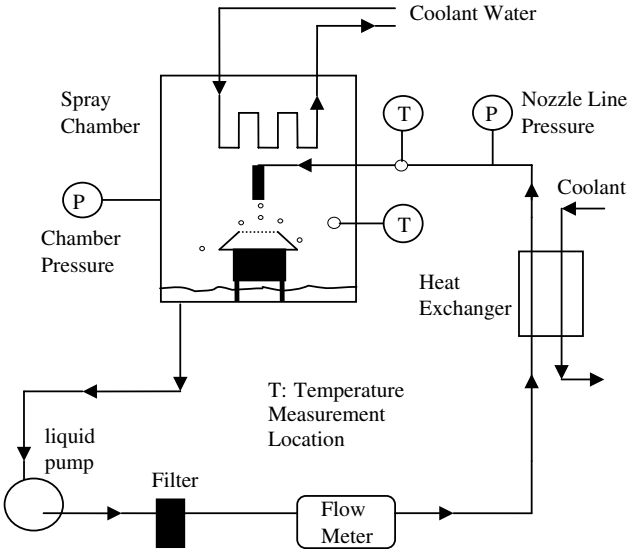

Fig. 1. Spray cooling test rig configuration.

(Fig. 2a). The upper section of the heater block was epoxied to the flange. The temperature distribution in the heater blocks were sampled using five T-type thermocouples mounted in the neck of each block (shown in Fig. 2b). The heat flux was calculated using Fourier's law of conduction assuming steady state 1-D conduction through the neck of the block. The reported heat flux was obtained by averaging the heat flux computed from neighboring thermocouple pairs. Surface temperature was determined by linear extrapolation of the temperatures indicated by TC1 and TC2.

2.2. Procedure

Prior to each test, the spray chamber and fluid loop were charged with PF-5060. A vacuum was repeatedly applied to the chamber until a pressure of 41.4 kPa (470 ppm gas concentration) was reached. The chamber was allowed to attain equilibrium prior to conducting the tests. All tests were run at constant chamber pressure, liquid flow rate (200 ml/min), and constant nozzle height (17 mm) above the heater surface. The nozzle height selected provided optimal spray coverage of the heated surface, while the liquid flow rate of 200 ml/min was the maximum the nozzle/pump could reliably supply. Test conditions for the working fluid are shown in Table 1. Heat was supplied to the cartridge heater in increments of 10 W using a programmable power supply. Steady state was achieved at each power level, and data acquired before the heat load was increased for the next sample point. CHF was detected by a rapid increase in the surface temperature with a simultaneous decrease in heat flux. The heater was designed to allow all tests to reach the CHF condition. Power to the cartridge heater was shut off when CHF was reached. The maximum heat flux shown in the spray cooling curves represents the last stable measurement prior to CHF.

2.3. Nozzle

A Parker Hannifin prototype spray nozzle (plate #7) was used for each of the tests. The nozzle consisted of a 2×2 array of pressure swirl atomizers with a spacing of 6 mm. Prior to heat flux testing, the spray nozzle

Table 1
Test case conditions

PF-5060 spray cooling parameters	
P_{sat}	41.4 kPa
T_{sat}	31 °C
T_l	20.5 °C
h_{fg}	92 kJ/kg

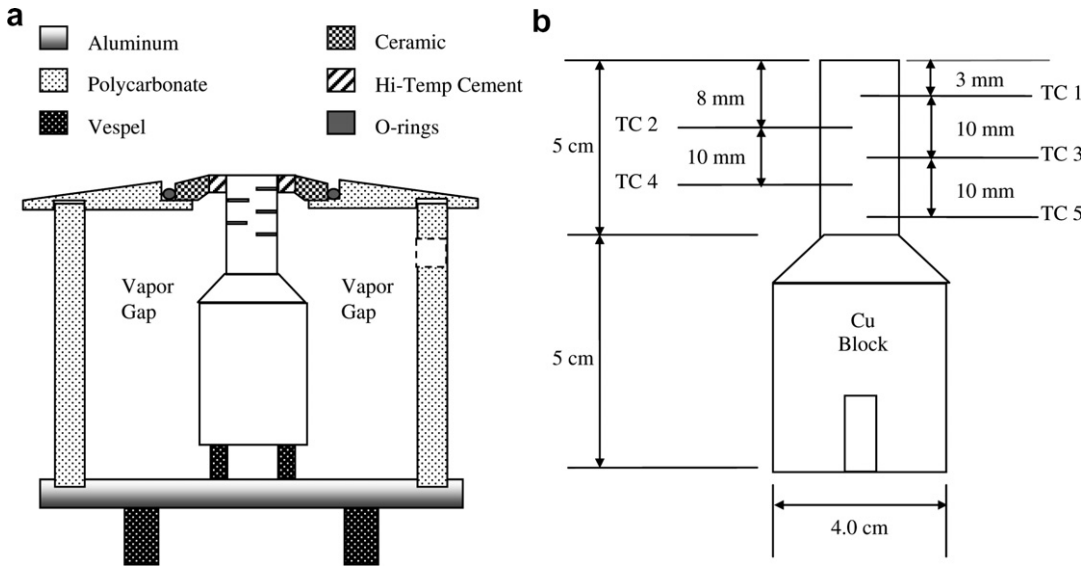

Fig. 2. Copper block schematic; (a) housing, (b) TC locations.

uniformity for the entire array was measured using several stainless steel tubes of different inner diameter, a graduated cylinder, and a stopwatch. The largest tube had an inner diameter approximately the same diameter as the heated surface. Size, local volume flux between concentric cylinders, and the local volume flux between concentric cylinders normalized by the volume flux averaged over the entire heater surface (Γ) is shown in Fig. 3. A Γ value of unity indicates that the local volume flux is identical to the average volume flux across the entire heater surface. The outer ring (A_4) is seen to have 60% less volume flux than the average value. The volume flux gradually increases towards the center of the spray. The center ring (A_1) has twice as much volume flux as the average flux for the entire area. The volume flux variation indicates the spray may be considered a non-uniform, center-biased spray. Although the volume flux appears qualitatively similar to that of a single-nozzle full-cone spray, one important difference due to the use of multiple nozzles is a non-radial momentum and mass flux in the region between the nozzles. This can result in the accumulation of fluid on the surface, especially when the standoff height is small relative to the nozzle spacing. Volume flux measurements were also obtained for each of the inclined sprays investigated using the largest tube from the concentric cylinder measurements. Detailed spray characteristics (droplet size, droplet velocity and spray density) were not obtained in this study.

Section	Area (cm^2)	Area (%)	Vol. Flux (m^3/m^2 s)	Γ_i
A_1	0.33	16.5	0.026	2.0
A_2	0.38	20	0.024	1.8
A_3	0.54	28.5	0.007	0.6
A_4	0.66	35	0.005	0.4

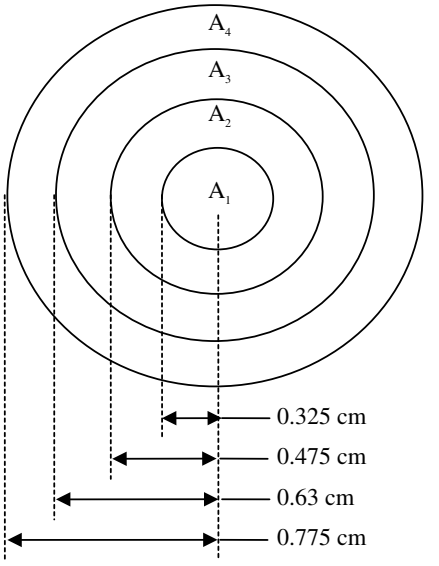

Fig. 3. 2×2 nozzle array impact upon spray uniformity.

2.4. Enhanced surfaces

The dimensions of the enhanced surface geometries studied are shown in Fig. 4a. The block labeled 1f corresponds to the flat surface (no fins present), 1p corresponds to the pyramid surface, 1c corresponds to the cubic pin finned surface, and 1s corresponds to the straight finned surface. Photographs of the enhanced surfaces are shown in Fig. 4b. X, L and H are the structure feature width, separation distance, and height, respectively. The separation distance for the pyramid surfaces' structures was zero (i.e, $L = 0$) because the structures were positioned immediately next to one another.

2.5. Spray inclination angle

Spray inclination angles (θ) were defined as the angle between the spray axis and the normal to the heated surface (Fig. 5). The four angles tested in this study were $\theta = 0°$ (vertical), 15°, 30°, and 45°. When spraying onto the straight fin surface at an angle other than $\theta = 0°$, the fin orientation relative to the spray axis must also be defined. Two orientations were tested in this study (Fig. 6); $\gamma = 0°$ (axial orientation) and $\gamma = 90°$ (transverse orientation). The nozzle manifold height (l) was held constant for each of the tests. Delrin spacers were fabricated

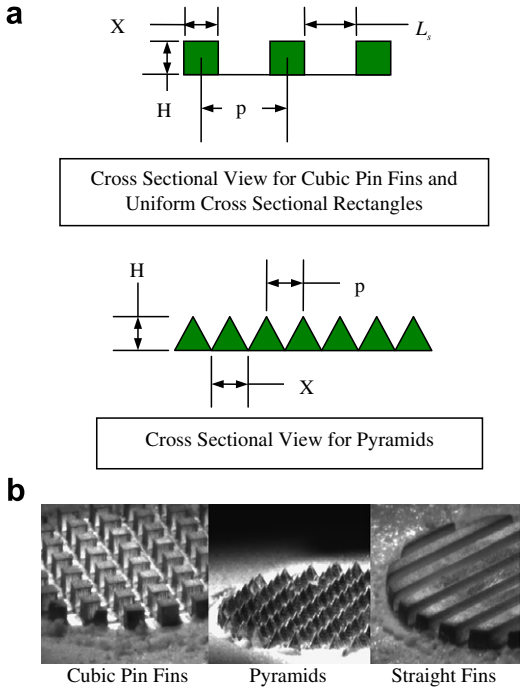

Surface	p (mm)	X (mm)	L (mm)	H (mm)	A_{surf} (cm^2)
Cubic Pin Fins (1c)	2	1	1	1	4.0
Straight Fins (1s)	2	1	1	1	4.0
Pyramids (1p)	1	1	0	1	4.5

Fig. 4. Enhanced surfaces; (a) geometry cross-sectional view, (b) CCD images.

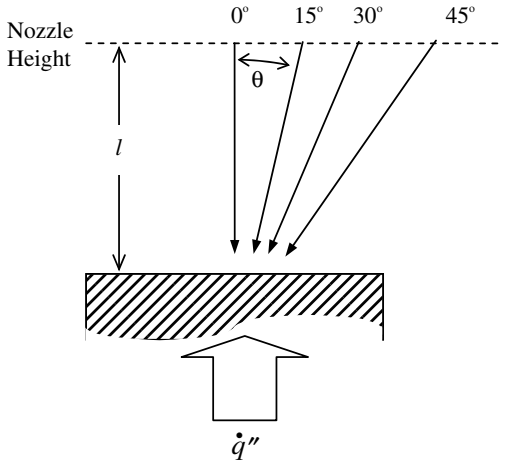

Fig. 5. Centerline axis trajectory survey angles.

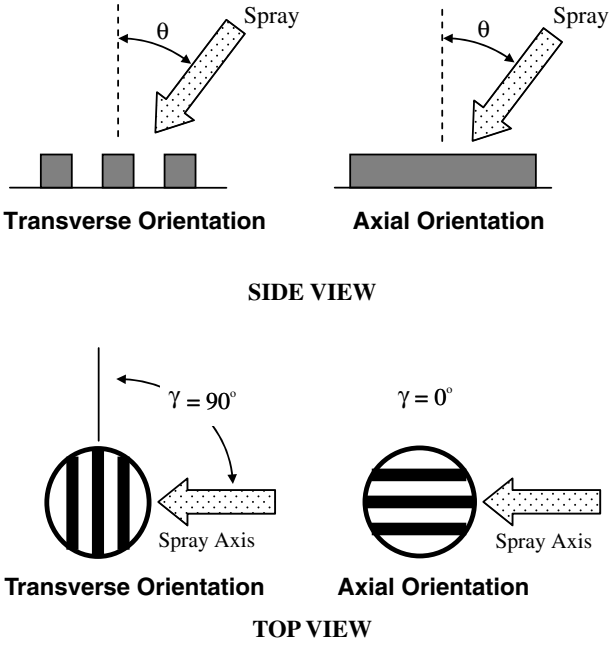

Fig. 6. Spray orientation relative to the straight fins.

and used to accurately position the nozzle relative to the heater surface. A spray angle of $\theta = 0°$ was used for each surface in the initial surface structure geometry survey.

2.6. Measurement uncertainty

The primary quantity of interest for these experiments is the heat flux, which has three sources of error: the thermal conductivity of the heater, the location of the thermocouples, and the error in the temperature measured. The conductivity value used was 389 ± 4 W/m K. The error in the thermocouple temperature measurements were approximately ± 0.5 °C. The error in the thermocouple location was determined to be ± 0.56 mm. Error for the reported heat flux values were calculated using Eq. (1).

$$\delta \dot{q}'' = \pm \sqrt{\sum_{j=1}^{N} \left[\frac{\left(\frac{\partial \dot{q}''_j}{\partial x}\delta_x\right)^2 + \left(\frac{\partial \dot{q}''_j}{\partial k}\delta_k\right)^2 + \left(\frac{\partial \dot{q}''_j}{\partial (\Delta T)}\delta_{\Delta T}\right)^2}{N^2} \right]} \quad (1)$$

The uncertainty in the heat flux was determined to be 5.6% at 80 W/cm^2. Analytical calculations showed that heat losses within the upper portion of the copper block to the ceramic flange was less than 1% of the total heat input at CHF for the flat surface case. An energy balance on the copper block indicated that the power removed by the spray was typically 93% of the power input to the cartridge heater. The heat flux demonstrated a repeatability within 1% for multiple tests under identical conditions. Pressures were measured within ±3 kPa, while flow rates measured had an error of ±1 ml/min.

3. Results and discussion

3.1. Structured geometry results

Spray cooling has been observed to be a convective boiling process that is largely dominated by single phase convection [23,24]. The enhanced structures used in this study can be considered finned heat sinks. Addition of finned heat sinks to convectively cooled surfaces is known to decrease the single phase convective thermal resistance (R_{fl}) to heat transfer [25] by increasing the total wetted area. If the heat flux were to scale with the total wetted surface area, then it would be expected that the pyramid surface would have the highest heat flux, followed by the cubic pin finned and straight finned surfaces, respectively.

The spray cooling curves for the enhanced geometry survey are shown in Fig. 7. All heat flux data are based on the projected area of 2.0 cm^2, instead of the wetted area. Table 2 summarizes the total wetted surface area (A_{surf}), CHF, CHF enhancement relative to the flat surface, area

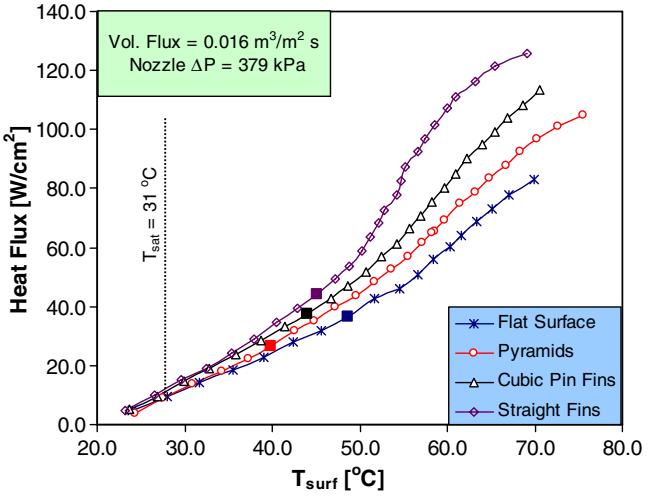

Fig. 7. Heat flux as a function of surface temperature and surface structure. *The approximate onset of multiphase effects is indicated by a solid square plot point on each curve.

Table 2
Summary of surface structure survey test data

Geometry	Surface	A_{surf} (cm^2)	γ (deg)	θ (deg)	q''_{CHF} (W/cm^2)	CHF enhancement (relative to flat surface CHF at $\theta = 0°$) (%)	Area utilization factor		T_{max} (°C)	$\eta_{2-\Phi}$ (%)
							$\xi_{1-\Phi}$ [b]	$\xi_{2-\Phi}$		
Feature geometry study										
Flat	1f[a]	2.0	–	0	80	0	–	–	70.0	29
Cubic pin fins	1c	4.0	–	0	114	43	0.52	0.73	70.6	41
Straight fins	1s	4.0	–	0	126	58	0.60	0.79	69.1	46
Pyramid	1p	4.5	–	0	105	31	0.32	0.58	75.6	38
Spray angle study										
Flat	1f[a]	2.0	–	0	80	0	–	–	70.0	29
Flat	1f[a]	2.0	–	15	98	23	–	–	70.5	36
Flat	1f[a]	2.0	–	30	96	20	–	–	67.4	35
Flat	1f[a]	2.0	–	45	92	15	–	–	67.8	33
Flat	1f[a]	2.0	–	0	80	0	–	–	70.0	29
Straight fins	1s	4.0	–	0	126	58	0.60	0.79	69.1	46
Straight fins	1s	4.0	0	15	131	64	0.60	0.82	70.0	48
Straight fins	1s	4.0	0	30	132	65	0.60	0.83	69.8	48
Straight fins	1s	4.0	0	45	126	58	0.60	0.79	66.7	46
Straight fins	1s	4.0	90	15	126	58	0.60	0.79	69.9	46
Straight fins	1s	4.0	90	30	140	75	0.60	0.88	70.5	51
Straight fins	1s	4.0	90	45	135	69	0.52	0.84	70.3	49

[a] Denotes that the area utilization factor is not applicable because area addition has not occurred.
[b] Single phase enhancement factor ratios were taken with heat flux values at the end of the single phase regime.

utilization factor (ξ), surface temperature at CHF for each of the blocks tested, and the evaporation efficiency as defined in Eq. (2). The area utilization factor (AUF) is defined as the ratio of the heat flux enhancement to the proportional increase in wetted area. AUF was computed for both the single phase regime ($\xi_{1-\Phi}$) and the multiphase regime at CHF ($\xi_{2-\Phi}$). The end of the single phase regime is the point at which multiphase effects (i.e. boiling) become pronounced. This is most noticeable in the heat flux curves at the point in which the relationship between the heat flux and the wall-to-spray temperature becomes non-linear. The AUF values in Table 2 were calculated relative to the flat surface case.

$$\eta_{2-\Phi} = \frac{\dot{q}''_{CHF}}{\dot{m}(c_p \Delta T + h_{fg})} \tag{2}$$

3.1.1. Single phase regime

At low heat fluxes (<45 W/cm^2), the heat transfer is dominated by single phase convection, resulting in a linear relationship between the heat flux and the wall-to-spray temperature difference as observed for all four geometries shown in Fig. 7. Performance of the enhanced surfaces all exceeded that of the flat surface. The straight finned surface had the smallest convective thermal resistance (as indicated by its largest slope), followed by larger thermal resistances for the cubic pin finned and the pyramid surfaces. The single phase AUF ($\xi_{1-\Phi}$) shown in Table 2 indicated similar trends.

3.1.2. Multiphase regime

Each of the enhanced surfaces transitioned into the multiphase regime at lower temperatures than for the flat surface (see Fig. 7), as indicated by the decrease in temperature of the point where the curve undergoes a distinct increase in slope. This may be due to an increase in the number of potential nucleation sites due to increased wetted area, or a longer residence time as the liquid traveled over the structure. Suppression of nucleation sites is known to occur during forced convection boiling heat transfer due to a thinning of the thermal boundary layer [26]. However, a decrease of the liquid velocity due to increased flow resistance by the structures may diminish such effects in spray cooling. Liquid pooling or lower liquid velocities may have occurred on parts of the fins that were shaded from the impinging droplets, allowing nucleation to occur more easily.

Heat flux performance in the multiphase regimes for the enhanced surfaces was consistently higher than on the flat surface. The straight finned surface had the highest heat transfer performance, followed by the cubic pin fins and the pyramids. The multiphase AUF ($\xi_{2-\Phi}$) showed similar trends. CHF for the pyramids, cubic pin finned, and straight finned surfaces were greater than for the flat surface by approximately 24, 33, and 46 W/cm^2 (58% increase for straight fins), respectively. The temperatures at which CHF occurred were within an 8 °C range. The enhanced surfaces had significantly higher evaporation efficiency than the flat surface (see Table 2).

3.1.3. Enhancement effects

To obtain a better understanding of the results, the total wetted surface area and the efficiency with which it is utilized should be considered. The data indicates that the heat transfer does not scale directly with the total wetted surface area in any of the heat flux regimes (both the straight fins

and cubic pin fins outperformed the pyramids which had the largest surface area). The greatest insight into surface structure effects can be gained by comparing the straight finned and cubic pin finned surfaces. Although the cubic pin fins and straight fins had the same total wetted surface area, there was a significant difference in the heat transfer performance. The difference must be a result of either liquid management on the heater surface, the efficiency with which the wetted area is utilized, or a combination of both.

3.2. Spray inclination angle results

3.2.1. Flat surface

Spray cooling curves for the flat surface (1f) are shown in Fig. 8a. Heat flux as a function of surface temperature and spray angle for the straight finned surface in the $\gamma = 0°$ and $\gamma = 90°$ orientations are shown in Fig. 8b and c. Fig. 8a shows that the heat flux increased as the spray angle increased from $\theta = 0°$ for the flat surface. The highest CHF of 98 W/cm^2 (23% enhancement relative to $\theta = 0°$) occurred for $\theta = 15°$. The $\theta = 45°$ case showed good agreement with the $\theta = 0°$ case in the single phase regime ($T_{surf} \leqslant 55$ °C). However, heat flux performance for the $\theta \geqslant 15°$ cases agreed within the experimental uncertainty in all heat flux regimes. The maximum surface temperature reached for $\theta = 15°$ was approximately the same as for $\theta = 0°$($T_{surf} \approx 70$ °C) while the other cases reached an approximate surface temperature value of 67 °C.

3.2.2. Straight finned surface

Results of the straight fin $\gamma = 0°$ study are shown in Fig. 8b. The heat flux curves for the $\theta = 0°$, 15°, 30°, and 45° cases agreed within the experimental uncertainty, indicating surprisingly little influence of spray inclination angle on the heat flux. All cases had a CHF value of approximately 132 W/cm^2. Results of the straight fin $\gamma = 90°$ study are shown in Fig. 8c, and indicate that spray inclination angle has a small effect on spray cooling for this orientation. The highest CHF occurred for $\theta = 30°$ (140 W/cm^2) with heat flux enhancements of 11% relative to the $\theta = 0°$ case and 75% relative to the $\theta = 0°$ flat surface case. The 45° case had a CHF value (135 W/cm^2) slightly lower than the 30° case. The $\theta = 15°$ case had the same CHF as the 0° case (126 W/cm^2). The heat fluxes for each of the straight fin cases agreed within the experimental uncertainty in both the single phase and multiphase regimes. Separation of the curves did not occur until just before CHF. CHF for $\theta = 30°$ was higher than the $\theta = 0°$ and $\theta = 15°$ cases.

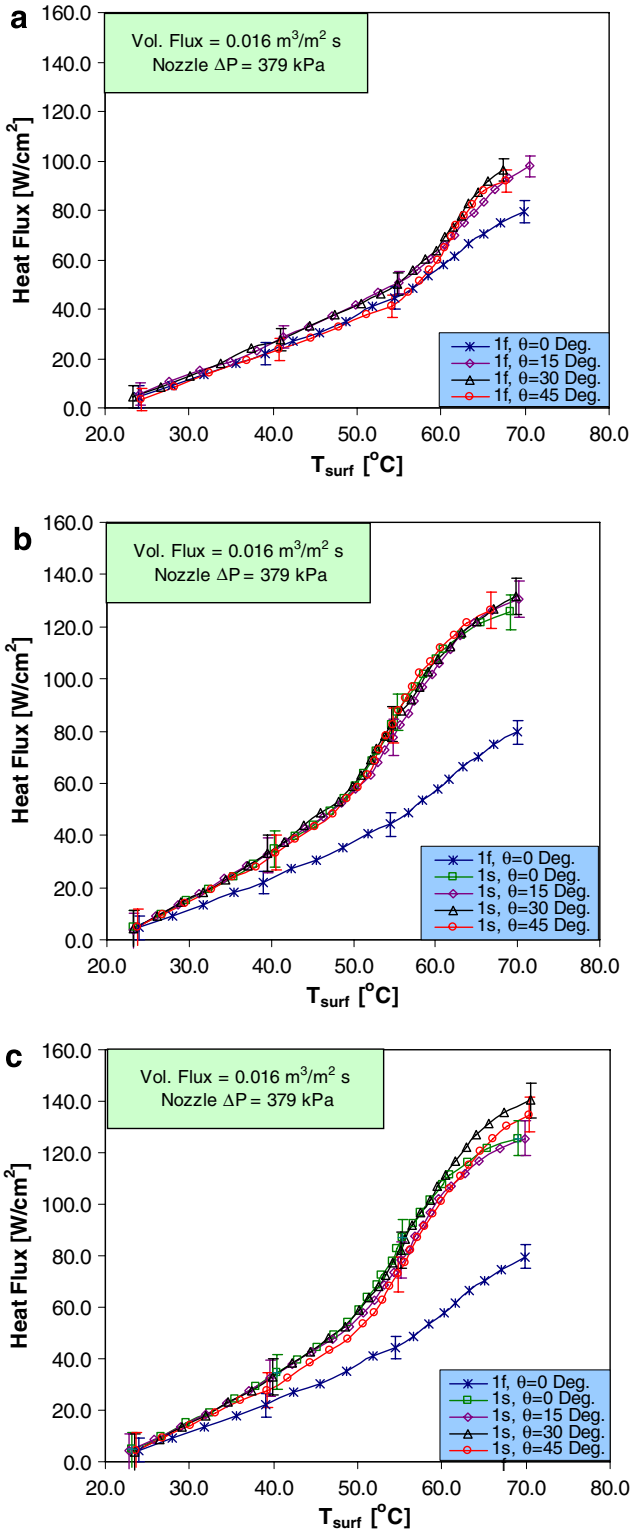

Fig. 8. Heat flux as a function of surface temperature and trajectory angle; (a) flat surface, (b) axial straight fins ($\gamma = 0°$), (c) transverse straights fins ($\gamma = 90°$).

3.3. Discussion

3.3.1. Structured geometry enhancement mechanisms

Due to the highly complicated nature of the spray/surface interaction and the inability to make local heat transfer and film characteristics measurements on enhanced surfaces, a definitive explanation of the observed results cannot currently be given. Even on smooth surfaces, the mechanisms by which heat is removed during spray cooling is not well understood due to the inability to independently control drop size, drop velocity, and mass flux.

One proposed mechanism is that the spray produces a thin film on the surface through which conduction occurs. The thinner the film, the higher the heat transfer [2,4,10]. In another proposed mechanism, boiling is thought to occur in the liquid film. The growing bubbles, however, are punctured by the incoming droplets before they can grow to appreciable size. The growth and collapse of many small, rapidly growing bubbles was proposed to be the dominant heat transfer mechanism [15]. Previous work by the authors has found that the heat transfer scales directly with the length of the three-phase contact line [16,27], implying that the mechanism may be governed by transient conduction into a highly disrupted film or by evaporation at the contact line [26].

The efficiency with which the added surface area is used is strongly dependent on the enhanced structure geometry. This can be quantified by the AUF as presented in Table 2. For all cases, AUF values smaller than unity were observed, indicating the heat transfer does not scale in proportion to the wetted area. In both the single phase and multiphase regimes, the straight finned surface had higher AUF values than the cubic pin fin and pyramid surfaces (Fig. 7).

Some of the methods by which the addition of enhanced surfaces affects the thermophysics of spray evaporation are briefly discussed. The addition of enhanced surface geometries greatly modifies the nature of the fluid/solid contact. The relative increase in wetted surface area can be expected to increase frictional resistance thereby retarding the fluid motion. The longer liquid residence time on the heater surface can allow for more heat exchange through increased sensible heating of the liquid. It can also increase the multiphase contribution by providing many more nucleation sites, and allow activation of these nucleation sites at lower wall temperatures as mentioned above. If enhanced surfaces affected the thermophysics in only these two ways, however, the cubic pin finned surface would be expected to have higher heat transfer than the straight finned surface. The fact that the highest AUF value occurred for the straight finned case, however, suggests that other factors affect the heat transfer.

For a convectively dominated process, the heat transfer is determined by the heat transfer coefficient, the wetted area, and the surface-to-fluid temperature difference. Since the temperature difference ($T_{surf} - T_l$) and the wetted area of the cubic pin finned surface and the straight finned surface were identical, differences in the heat transfer performance between these surfaces must be due to differences in the heat transfer coefficient. The heat transfer coefficient for the straight finned surface might be expected to be higher than for the cubic pin finned surface based on the following reasoning. If it is assumed that all liquid sprayed onto the surface flows between the structures before leaving the surface, then the cubic pin finned surface has twice the cross-sectional area available to drain the fluid compared to the straight finned surface. The liquid velocities on the straight finned surface would be expected to be twice as high, resulting in a larger heat transfer coefficient.

3.3.2. Inclination enhancement mechanisms

The increase in heat transfer with inclination angle observed in the current results is not consistent with those of previous studies which indicated minimal impact of inclination angle [22]. The reason for this might be attributed to

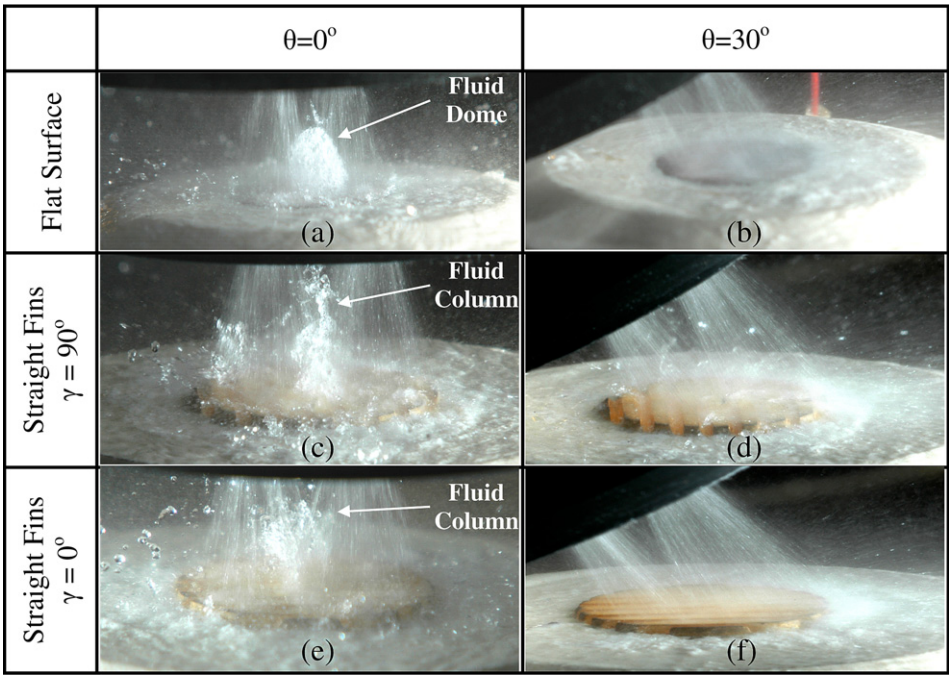

Fig. 9. Spray cone stagnation zone phenomena; (a) $\theta = 0°$ flat surface, (b) $\theta = 30°$ flat surface, (c) $\theta = 0°$, transverse straight fins ($\gamma = 90°$), (d) $\theta = 30°$, transverse straight fins ($\gamma = 90°$), (e) $\theta = 0°$, axial straight fins ($\gamma = 0°$), (f) $\theta = 30°$, axial straight fins ($\gamma = 0°$).

the particular spray nozzle used in this study. As mentioned earlier, the 2×2 Parker Hannifin spray manifold used for these studies created a stagnation zone in the center of the heated surface, resulting in the accumulation of an unsteady liquid pool in the center of the heater surface for $\theta = 0°$ on both the flat and straight fin surfaces (Fig. 9). As heat fluxes increased towards CHF, the amount of accumulated liquid visibly diminished. For the inclined sprays ($\theta = 15°$, 30° and 45°), however, pooling was not noticed in any of the heat flux regimes, indicating that the inclined sprays promoted better liquid drainage from the heated surface through elimination of the stagnation zone, and may have been the reason for the increased heat transfer.

As the inclination angle was increased, the volumetric flux of liquid striking the surface decreased as a result of overspray, which might be expected to cause a decrease in heat transfer. Volume flux measurements were obtained at each of the inclination angles tested. The measurements showed that the liquid captured at the $\theta = 15°$ inclination was approximately equal (within 2%) to that captured at $\theta = 0°$. The liquid captured at the $\theta = 30°$ and $\theta = 45°$ inclination, however, were reduced by 8% and 15%, respectively. Since flat surface CHF values for the inclined sprays showed better performance relative to the $\theta = 0°$ case, and the CHF values for the straight finned surface cases were comparable for all angles, it may be possible that keeping the volumetric flux constant as the inclination angle increased would have provided even higher enhancement. These results have implications when using multi-nozzle arrays to cool large flat surfaces requiring additional nozzles for full liquid coverage. An inclined spray axis can be used to produce a net momentum flux to sweep any stagnant pooled regions off the surface thereby mitigating heat flux reduction due to stagnation zone phenomena.

4. Conclusions

Spray cooling heat flux measurements were performed on three enhanced surfaces (cubic pin fins, pyramids, and straight fins) and one flat surface using PF-5060. Tests were performed using degassed fluid at 41.4 kPa. The volumetric flow rate (0.016 m^3/m^2 s) and nozzle height from the surface were held constant for all the tests.

From the surface geometry survey, CHF values of 80 W/cm^2, 114 W/cm^2, and 105 W/cm^2 were attained for the flat, cubic pin finned, and pyramid surfaces, respectively. The straight finned surface had the highest performance, and reached a CHF value of 126 W/cm^2. Multiphase efficiencies for the pyramid, cubic pin finned, and straight finned surfaces were 38%, 41%, and 46%, respectively, compared to an efficiency of 29% for the flat surface. Heat flux enhancement was observed in both the single phase and multiphase regimes. This work extends the work of Pais et al. [10] and Sehmbey et al. [6] by showing that heat flux can be enhanced by spraying structured surface geometries significantly larger than the film thickness.

From the inclined spray results, it was shown that spray angles greater than 15° eliminated the excess liquid on the heater surface due to the multi-nozzle array stagnation zone phenomena. A maximum heat flux of 140 W/cm^2 was attained with the straight fin surface spray orientation at $\gamma = 90°$, $\theta = 30°$, giving an enhancement of 75% relative to the flat surface case at the vertical spray orientation ($\theta = 0°$). Although the volume flux on the heater surface decreased with increasing inclination angle, the heat flux increased, indicating that the enhancements were likely a result of altered film drainage from the surface.

The current results illustrate that the use of an enhanced heating surface presents a simple, passive method to improve the thermal performance of spray cooling. Furthermore, this benefit is realized without significant penalty, in contrast to other control parameters (such as mass flow rate or subcooling) which can be expensive in terms of pump power, cost, and weight. The high efficiencies that were attained in this study using simple, non-optimized geometries indicate that even further increases in wall heat transfer might be attained once the surface geometry is optimized.

Acknowledgements

Eric A. Silk was supported by the Thermal Management group of the Laboratory for Physical Sciences and funded by the Laser Risk Reduction Program (LRRP) at the NASA Goddard Space Flight Center. Dr. Jungho Kim and Dr. Kenneth Kiger would like to acknowledge the generous support of the Office of Naval Research under Contract Number N000140410315 directed by Dr. Mark Spector. The authors would like to thank Dr. Paul Boudreaux, for his assistance, as well as J.B. Dotellis and Lester Lorentz for their support in machining the copper test articles and their surfaces. Special thanks is given to Mario Martins, Alice Rector, Jim Dye, Mark Kobel, Rick Fedorchak and Richard Freburger of NASA Goddard Space Flight Center for their test support. Thanks is also given to Eric Golliher of NASA Glenn Research Center for his insights into the history of the Shuttle Program. Parker Hannifin's Gas Turbine Fluid Systems Division (GTFSD) generously supplied the spray nozzle.

References

[1] M. Sehmbey, L. Chow, M. Pais, T. Mahefkey, High heat flux spray cooling of electronics, in: 12th Symposium on Space Nuclear Power and Propulsion, Albuquerque, NM, January, AIP Conference Proceedings No. 324, 1995, pp. 903–909.
[2] J. Yang, M. Pais, L. Chow, Critical heat flux limits in secondary gas atomized liquid spray cooling, Exp. Heat Transfer 6 (1993) 55–67.
[3] K.A. Estes, I. Mudawar, Correlation of Sauter mean diameter and critical heat flux for spray cooling of small surfaces, Int. J. Heat Mass Transfer 38 (16) (1995) 2985–2996.
[4] J. Yang, L. Chow, M. Pais, Nucleate boiling heat transfer in spray cooling, J. Heat Transfer 118 (1996) 668–671.

[5] R.-H. Chen, L. Chow, J. Navedo, Effects of spray characteristics on critical heat flux in subcooled water spray cooling, Int. J. Heat Mass Transfer 45 (2002) 4033–4043.
[6] M. Sehmbey, M. Pais, L. Chow, A study of diamond laminated surfaces in evaporative spray cooling, Thin Solid Films 212 (1992) 25–29.
[7] W. Healy, P. Halvorson, J. Hartley, S. Abdel-Khalik, A critical heat flux correlation for droplet impact cooling at low Weber numbers and various ambient pressures, Int. J. Heat Mass Transfer 41 (1998) 975–978.
[8] M. Sawyer, S. Jeter, S. Abdel-Khalik, A critical heat flux correlation for droplet impact cooling, Int. J. Heat Mass Transfer 40 (9) (1997) 2123–2131.
[9] J.D. Bernadin, I. Mudawar, The Leidenfrost point: experimental study and assessment of existing models, J. Heat Transfer 121 (1999) 894–903.
[10] M. Pais, L. Chow, E. Mahefkey, Surface roughness and its effects on the heat transfer mechanism of spray cooling, J. Heat Transfer 114 (1) (1992) 211–219.
[11] I. Mudawar, K. Estes, Optimizing and predicting CHF in spray cooling of a square surface, J. Heat Transfer 118 (1996) 672–679.
[12] Y.M. Qiao, S. Chandra, Experiments on adding a surfactant to water drops boiling on a hot surface, Proc. R. Soc. London 453 (1997) 673–689.
[13] Y. Qiao, S. Chandra, Spray cooling enhancement by addition of a surfactant, J. Heat Transfer 120 (1998) 92–98.
[14] R. Mesler, Surface roughness and it's effects on the heat transfer mechanism of spray cooling, J. Heat Transfer 115 (1993) 1083–1085.
[15] D. Rini, R.-H. Chen, L. Chow, Bubble behavior and nucleate boiling heat transfer in saturated FC-72 spray cooling, J. Heat Transfer 124 (2002) 63–72.
[16] B. Horacek, K. Kiger, J. Kim, Single nozzle spray cooling heat transfer mechanisms, Int. J. Heat Mass Transfer 48 (8) (2005) 1425–1438.
[17] J.R. Nason, F. Wierum, J. Yanosy, Challenges in the development of the orbiter active thermal control subsystem, in: NASA Johnson Space Center Space Shuttle Technical Conference Proceedings, Houston, TX, January 1985, pp. 450–464.
[18] H. Honda, H. Takamastu, J.J. Wei, Enhanced boiling of FC-72 on silicon chips with micro-pin-fins and submicron-scale roughness, J. Heat Transfer 124 (2002) 383–390.
[19] L.H. Chien, R.L. Webb, A parametric study of nucleate boiling on structured surfaces, Part I: Effect of tunnel dimensions, J. Heat Transfer 120 (1998) 1042–1048.
[20] T.A. Shedd, A.G. Pautsch, Full Coverage spray drainage system and method for orientation-independent removal of high heat flux, U.S. Patent Pending, 2005.
[21] D. Kearns, J.H. Du, R.H. Chen, L. Chow, A Parametric study of dielectric spray cooling of a row of heaters in a narrow channel, in: 18th IEEE SEMI-THERM Symposium, San Jose, CA, Conference Proceedings, March 12–14, 2002.
[22] J. Schwarzkopf, G. Sovar, T. Cader, K. Okamoto, B.Q. Li, B. Ramaprian, Effect of spray angle in spray cooling thermal management of electronics, in: ASME Heat Transfer/Fluids Engineering Summer Conference, Charlotte, NC, Conference Proceedings, July 11–15, 2004.
[23] E.A. Silk, J. Kim, K. Kiger, Investigation of enhanced surface spray cooling, in: ASME International Mechanical Engineering Congress, Anaheim, CA, IMECE2004 Conference Proceedings, November 13–19, 2004.
[24] E.A. Silk, J. Kim, K. Kiger, Impact of cubic pin finned surface structure geometry upon spray cooling heat transfer, in: ASME International Electronic Packaging and Technical Conference, San Francisco, CA, InterPACK 2005 Conference Proceedings, July 17–22, 2005.
[25] A.D. Krause, A. Bar-Cohen, Design and Analysis of Heat Sinks, John Wiley & Sons Inc., New York, 1995, pp. 11–28.
[26] M. Potash Jr., P.C. Wayner Jr., Evaporation from a two-dimensional extended meniscus, Int. J. Heat Mass Transfer 15 (1972) 1851–1863.
[27] B. Horacek, J. Kim, K. Kiger, Spray cooling using multiple nozzles: visualization and wall heat transfer measurements, IEEE Trans. Dev. Mater. Reliab. 4 (4) (2004) 614–625.